Investigation of Liquid Fuel Injection Processes in a Rotating Detonation Combustor using Megahertz Planar Laser-Induced Fluorescence Imaging

Matthew Hoeper[a], Austin M. Webb[a], Venkat Athmanathan[a], Bebe Wang[a], H. Douglas Perkins[b], Sukesh Roy[c], Terrence R. Meyer[a,d], Christoper A. Fugger[c]

[a] *School of Mechanical Engineering, Purdue University, IN, 47907, USA*
[b] *NASA Glenn Research Center, Cleveland, OH 44135, USA*
[c] *Spectral Energies LLC, Beavercreek, OH, 45430, USA*
[d] *School of Aeronautics and Astronautics (by courtesy), Purdue University, IN, 47907, USA*

Abstract

Direct imaging of liquid fuel injection is performed within an optically accessible rotating detonation combustor (RDC) using planar laser-induced fluorescence (PLIF) to spatio-temporally resolve the highly dynamic spray characteristics at rates up to 1 MHz. The RDC is operated on air and hydrogen to sustain a stable, cyclically propagating detonation wave with cycle periods of up to $\sim$250 μs. One of the hydrogen fuel injection sites is replaced with a liquid jet to introduce a diesel spray as a fuel surrogate to enable tracer-free fluorescence excitation using the 355 nm third-harmonic output of a burst-mode Nd:YAG laser. The time-resolved PLIF measurements reveal the evolution of the highly unsteady spray, including the dwell period after the arrival of the detonation wave, the jet recovery, breakup and entrainment into the supersonic crossflow of air, propagation into the detonation chamber, and interaction with the detonation wave. Following passage of the detonation wave, the spray characteristics reveal significant changes in the momentum flux ratio between the liquid and air streams, altering the jet trajectory and temporarily halting fuel delivery to the detonation channel. This temporary cessation of fuel spray injection into the combustor is quantified, along with the fill rate as a function of time. As the injection system recovers, the fuel spray eventually returns to a quasi-steady position prior to the arrival of the detonation wave, allowing qualitative comparisons with theoretical jet trajectories for a range of air mass-flux conditions. These data, enabled by ultra-high-speed PLIF imaging, represent some of the first detailed measurements for characterizing and quantifying the interactions of liquid jets and detonations in an operating RDC.

Keywords: rotating detonation combustor; rotating detonation engine; fuel spray; high-speed imaging; planar laser-induced fluorescence

1. Introduction

The Rotating Detonation Combustor (RDC) is of significant interest for its potential to further improve the thermodynamic efficiency and size form factor of air-breathing and rocket propulsion systems. For many RDCs currently being investigated, non-premixed reactants are injected at the inlet of a cylindrical annulus, and after fuel-oxidizer mixing, a detonation wave then propagates azimuthally around the annulus consuming the reactants. The combustion products expand and exit from the other end of the device. The result is a highly unsteady and periodic system, with detonation waves typically propagating at speeds of 1–2 km/s around the detonation channel. Hence, periodic reactant refill-combustion cycle times of $\sim$30-1000 μs can occur for single or multiple detonation wave cases, with large and rapid pressure and temperature increases resulting from the approximately isochoric heat release. Other potential secondary shock wave phenomena can also affect the reactant dynamics and local temperatures and pressures within the system.

Although the RDCs represent a promising new approach, a technology feasibility assessment is difficult to perform as many of the gas dynamic, combustion, and coupled effects are not yet well understood, particularly for the case of liquid-based systems that also include multiphase phenomena. For fuel and oxidizer injection processes, the periodic high-pressure detonation impulses lead to highly unsteady reactant inlet dynamics, greatly affecting the combustor flowfield. The majority of prior RDC studies have been on gas-gas RDCs. Based on numerical simulations and limited experimental measurements, RDC behavior includes reactant injection cessation into the combustor channel for as much as 25% of the detonation period [1], unequal injection recovery times of the fuel and oxidizer, non-ideal reactant mixing, and reactant mixing with combustion products [2]. These effects may then lead to deflagration upstream of the detonation wave and incomplete burning of the fuel. Resolving these processes experimentally and determining cause and effect are inherently difficult as they occur on timescales smaller than the cyclical detonation passage, and detailed in-situ measurements with high spatio-temporal resolution have been relatively limited in RDCs thus far, particularly for liquid-based systems.

Studies with liquid injection in RDCs are typically motivated by the development of practical propulsion systems and/or collection of operating characteristics for evaluation of models. Fundamental detonation/shock interactions with liquid injection have been investigated in linear channels with significant optical access. Studies of RDCs using liquid fuel injection in air have noted an overall reduced RDC operability [3, 4], whereby reactant enrichment with another more reactive species or reactant preheating improved performance. Bench-scale experiments of water jet-detonation wave interactions have visualized the liquid-jet temporal evolution in response to either one or two repeated detonation waves, quantifying the jet trajectory and recovery characteristics under elevated mean chamber operation conditions [5, 6]. An interesting conclusion from these studies was that even for high-pressure-drop liquid injectors, spray breakup, atomization, and mixing was not fully complete in a $\sim$100 μs time period, and they suggested that additional wave-based atomization/mixing processes likely played a role in liquid RDC operation.

The extent to which RDCs will continue to be improved relies on a better understanding of the behavior of liquid injection in a highly unsteady and impulsive environment. In an RDC, there is limited visualization (or direct measurement) of liquid injection reported in the literature, and even gas-gas RDC measurements of the propellant injection are still extremely limited [7]. The current work aims to provide direct imaging and elucidate key liquid injection dynamics in the presence of rotating detonations. The RDC is operated on air and hydrogen to sustain a stable, cyclically propagating detonation wave, and one of the hydrogen fuel injection sites is replaced with a liquid jet to introduce a diesel spray that can be visualized using burst-mode planar laser-induced fluorescence at unprecedented rates up to 1 MHz. First, the RDC operation and ultra-high-speed imaging diagnostics are introduced. This is followed by a phenomenological description of the fuel spray propagation into the combustor channel across a full detonation cycle. The detailed characteristics of the unsteady fuel spray are then quantified, including its trajectory prior to detonation wave arrival and its recovery time in response to the passage of the detonation wave.

2. Experimental Setup

2.1. Rotating Detonation Combustor

The RDC geometry and its general operation have been described in previous works and a brief description is provided here [8]. The RDC has a nominal diameter of 125 mm, a throat gap of 1.42 mm and a channel gap of 10.7 mm. The outer body is constructed of quartz for optical accessibility. The combustor uses air and hydrogen as primary reactants and flow rates are controlled with critical venturis located upstream of the RDC. Air flows through a plenum and then into a contraction section where a sonic condition is reached. The air accelerates to approximately Mach 2 then passes over a backwards facing step and into the combustion chamber. Hydrogen is injected radially in a jet-in-crossflow configuration via a distribution ring. The hydrogen injection occurs 1 mm axially downstream of the throat at which the air is traveling just above Mach 1. Detonation is initiated by a pre-detonator where a small volume that is filled with oxygen and hydrogen is spark ignited. The

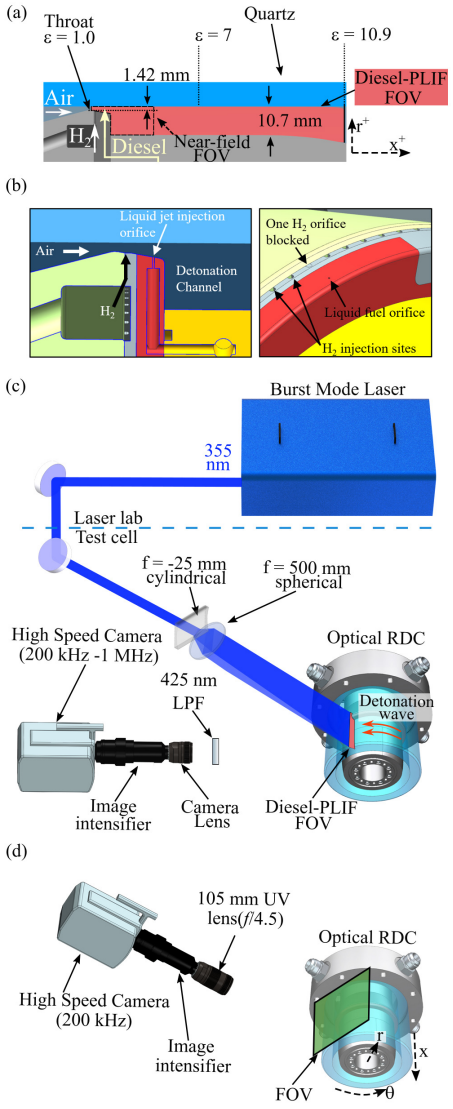

Fig. 1: (a) RDC cross-section view showing the detonation channel. (b) Enhanced injector views showing the the liquid fuel injector. (c) Laser and optical arrangement for the PLIF measurements. (d) Chemiluminescence camera arrangement.

pre-detonator is connected to the primary combustion chamber by a 3 mm diameter tube.

2.2. Liquid Fuel Jet

A single liquid diesel fuel jet is injected into the RDC. The overall air-hydrogen RDC sustains a cyclically propagating detonation wave. One of the hydrogen fuel injection sites is removed and replaced nearby with the orifice for the liquid fuel jet. As shown in Figure 1, this liquid fuel orifice is located at the same azimuth location as the blocked hydrogen orifice, but is located 4.1 mm axially downstream (though it's still within the injector). The internal geometry of the liquid fuel injector is cylindrical, with an orifice exit diameter of 0.3 mm with length to diameter ratio of 10. The liquid fuel orifice is fed by a 2 mm diameter plenum with a length of 13.7 mm. The liquid fuel is supplied to the plenum from internal passages within the RDC centerbody. The liquid flowrate is metered and controlled XX inches upstream of the liquid fuel plenum. The mass flow rate of liquid fuel is calculated from an average experimentally determined discharge coefficient of 0.26 and the pressure measurement upstream of the injector.

2.3. Laser System and Optical Arrangement

High-speed imaging of the liquid diesel jet was performed using 355-nm planar laser-induced fluorescence (PLIF) imaging simultaneous with broadband flame chemiluminescence imaging. The diesel PLIF is used to spatio-temporally resolve the fuel spray, and the chemiluminescence is used for tracking the detonation wave and combustion.

The use of diesel for PLIF has been reported for dynamic imaging of fuels prays in internal combustion engine environments at rates up to 50 kHz [9]. In the current work, a high-power burst-mode Nd:YAG laser was used to excite the diesel fuel in the detonation channel at rates up to 1 MHz. The fundamental wavelength of 1064 nm was frequency doubled to 532 nm and the remaining 1064 nm light was mixed with the 532 nm to generate 355 nm. The laser was operated at repetition rates of either 200 kHz or 1 MHz with typical burst lengths of 1500 µs and 750 µs, respectively. The 355 nm pulse energy used at 200 kHz was ∼4.5 mJ/pulse and ∼520 µJ/pulse at 1 MHz.

To resolve both small-scale and large-scale fuel spray features, two imaging schemes were implemented. The first imaging scheme was performed at 200 kHz repetition rate and for this case the PLIF imaged the entire length of the detonation channel (from the injector to the combustor exit plane). For this, a high-speed Phantom v2012 camera was paired with a high-speed Lambert HiCatt image intensifier, with a 85 mm $f/1.8$ visible camera lens, and a bandpass optical filter. For the chemiluminescence imaging, a

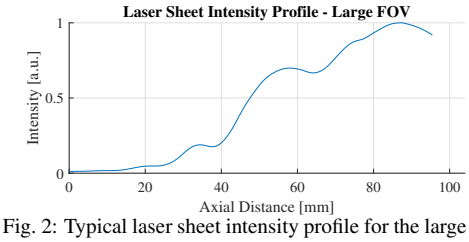

Fig. 2: Typical laser sheet intensity profile for the large FOV cases.

second high-speed Phantom v2012 camera was coupled with a high-speed UV intensifier (LaVision IRO) and a 105 mm UV f/4.5 camera lens.

The second imaging scheme was performed at a 1 MHz repetition rate and for this case the PLIF imaged a much smaller field of view (FOV), only extending approximately 16 mm axially downstream from the liquid fuel injection (15% of the length of the detonation channel). For this small FOV case, an ultra-high-speed Shimadzu HPV-X2 camera was used with a 200 mm f/4 lens, and a longpass optical filter. Combined with the dense spray, the laser fluence of the near-field imaging was sufficient to not warrant the use of an imaging intensifier.

The PLIF plane is a radial-axial plane at 45 degrees with respect to vertical plane. The chemiluminescence view is of a tangential plane that is centered on and perpendicular to the PLIF plane. For the large FOV imaging where the near-field (dense spray) and far-field (dispersed spray) were simultaneously imaged, the laser sheet intensity profile was tailored to have an axial distribution such that the laser energy was weakest in the near field and strongest in the far field, as shown in Figure 2

2.4. Operating Conditions

Six cases of RDC operation are considered with injection of the single liquid fuel jet, shown in Table 1. Cases 1, 2, and 3 hold air mass flow rate, hydrogen flowrate (and consequently Air-H2 equivalence ratio) constant while the liquid fuel flow rate is varied. As the liquid fuel injector pressure increases, the calculated liquid jet to air crossflow momentum flux ratio correspondingly increases. The momentum flux ratios are calculated from continuity based on the liquid orifice diameter and the annular area for the air at the liquid jet injection location. Cases 1 and 5 have similar liquid jet to air crossflow momentum flux ratios for different air mass flows. The nominal detonation wave speed is calculated as $\sim$85% of the Chapman-Jouguet condition. During hot fire operations, the RDC runs for 1 second. Liquid fuel injection begins at the same time as primary ignition and PLIF images are captured at t + 0.80 s.

3. Results and Discussion

3.1. Phenomenological Description of Spray Development

A phenomenological description of the injected liquid fuel jet and its evolution in the channel in time is provided to highlight the highly unsteady fuel spray behavior in response to the passage of the detonation wave. Figure 3 shows a diesel PLIF image sequence for Case 2 across one detonation period of the RDC. The image sequence begins in Figure 3 immediately prior to the arrival of a detonation wave, with the detonation wave propagating orthogonal to the PLIF plane (i.e., the detonation wave propagates in the theta direction as compared to the r-x PLIF plane). At 0 μs and 5 μs, the fuel spray is present across a large fraction of the combustor channel, with high concentrations of spray extending axially for approximately 60% of the combustor length. Sparse, but discernible, spray (low diesel PLIF signal) continues to be present moving closer to the channel exit, indicating either a lower concentration of diesel or the presence of smaller droplet sizes and/or evaporated gaseous diesel fuel. For x $<$ 30 mm, the spray is confined toward the outer radius of the channel, and for x $>$ 30 mm the spray expands rapidly to fill much of the channel radial width. This spray trajectory closely follows the outer contour of the wake formed behind the backward facing step [8], and thus indicates that the fuel spray is in immediate contact with the shear layer formed between the backward facing step wake and the in-flowing fresh reactants.

The detonation wave arrives between 5 μs and 10 μs and removes nearly all of the diesel within the combustor channel. Neaer the injector, the fuel spray is not removed and remains immediately outside of the diesel orifice, until about 60 μs, when the fuel spray begins to slowly enter the detonation channel. During this fuel spray recovery period ($\sim$10–60 μs), the fuel spray is not observed to significantly retreat back into the air injector. Gradually, the fuel spray begins refilling the detonation channel, beginning most noticeably near 80 μs. Early in the injector recovery (140–170μs), the near field (x$<$10 mm) shows an increased fuel spray penetration compared with times greater than $\sim$ 160 μs. This appears to indicate a more complete recovery of the air injection system (increasing the air momentum and thus decreasing the fuel spray penetration).

As the fuel spray fills the detonation channel, there are two regions with distinct spray patterns. The first region at x$<$20 mm captures the recovering fuel spray. This spray can be tracked from the fuel orifice beginning near 90 μs, indicating an in-plane (r-x) spray motion in the jet near field. The second region further downstream is most noticeable beginning in region C at 160 μs. As time progresses within region C, a large region of fuel spray begins to noticeably develop near 180 μs that continues to grow in size. The growth of this region and a second smaller region downstream are shown by the bounded dashed and dash-dot lines. The fuel spray in the second region does not correlate with in-plane spray convection as evidenced by tracking the leading edge of the near field spray refill process. This may indicate that the fuel in this region, beginning near x = 30 mm, originates from outside of PLIF plane. Since there is only a single liquid fuel jet, there are two explanations for the origin of the fuel spray in the far field region. First, the previous detonation cycle imparts an azimuth motion to the spray that is located outside of the r-x PLIF plane, and eventually this spray travels azimuthally to the PLIF measurement plane. A second explanation is that the observed region 2 fuel spray originates from the current refill period, and that the spray refill pro-

Table 1: Selected Test Conditions

Test Case	Air [kg/s]	Flow Rates Hydrogen [kg/s]	Liquid Fuel [g/s]	Equiv. Ratio	Mom. Flux Ratio	Liquid Fuel Inj. Pressure [bar]	Nom. Wave Speed [m/s]	Nom. Cycle Freq. [kHz]
1	0.46	0.012	0.92	0.91	0.055	16.0	1423	3.63
2	0.46	0.013	0.68	0.93	0.030	9.2	1420	3.63
3	0.45	0.012	0.43	0.93	0.012	4.3	1420	3.63
4	0.34	0.010	0.69	1.01	0.040	9.2	X	Y
5	0.22	0.005	0.67	0.85	0.059	8.5	1200	3.1

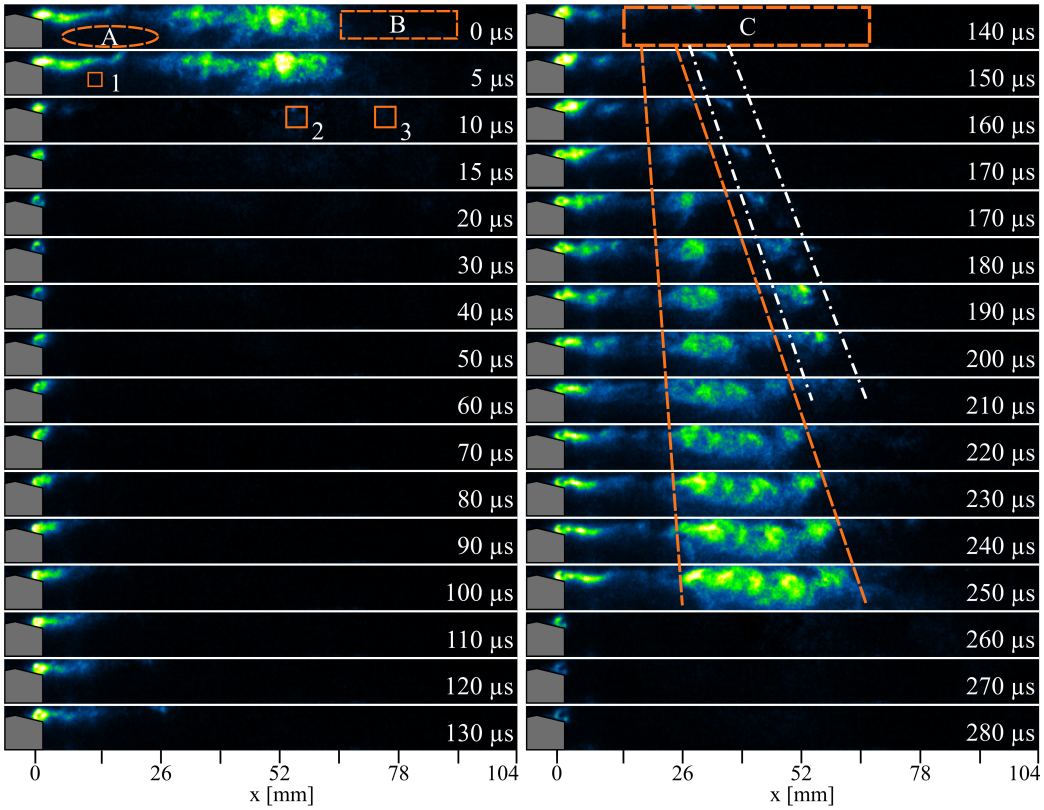

Fig. 3: Image sequence of diesel PLIF (large FOV, 200 kHz) for Case 2 across one period of the detonation wave passage.The first 6 frames are spaced 5 μs apart (the camera recording period), and the remaining frames are spaced by 10 μs for brevity.

cess occurs initially with a significant azimuth angle. This spray then gradually travels azimuthally back to the PLIF measurement plane. The significant increase in signal in the center of the combustor channel between 220 and 250 μs can be partially contributed to the large gradient in the laser sheet intensity profile shown in Figure 2. The location with the highest laser intensity is situated near the exit the of channel. It is possible that the lower signal between 10 and 26 mm is caused by a large drop in number density from the region near the injector exit, which is accompanied by low laser intensity, after which there is a rapid increase in laser intensity so the PLIF signal becomes significantly brighter as it moves downstream.

The smaller FOV imaging configuration provides enhanced spatial resolution to resolve the fuel spray temporal behavior. Figure 4 shows a 1 MHz PLIF image sequence of the near field fuel spray immediately before and following the detonation wave arrival. The orange lines represent the boundary of the spray. The boundary lines were calculated by defining the location at which the pixel intensity in every axial x position decays to 15% of the maximum intensity at that position. This calculation is performed twice; once to determine the upper spray boundary and once for the lower spray boundary. Similar to Figure 3, before

detonation wave arrival the near field spray is mostly confined to near the outer channel radius. Around 2 μs, the detonation wave arrives, and within 1 μs the majority of the fuel spray is removed. By 18 μs, the fuel spray is primarily in the radial direction outside of the orifice, and by 42 μs it is evident that the fuel spray trajectory begins again to curve downstream, indicating that air injection is beginning to recover. Similar to Case 2 in Figure 3, the spray is not observed axially far upstream of the liquid jet orifice site. Moreover, feature tracking near the liquid orifice suggests that the orifice is not turned off in response to the detonation wave and continues to flow liquid fuel into the injector (albeit at a slower rate) for the entirety of the detonation period.

A significant observation most apparent in the small FOV MHz-rate PLIF imaging is direct evidence of out-of-plane liquid motions. After a brief period following passage of the detonation wave, the liquid jet turns azimuthally towards the wave propagation direction; sometimes as much as 90 degrees relative to the axial direction. The out-of-plane diesel provides enough blockage to the PLIF object plane to produce a shadow effect on the out of plane diesel that allows out of plane motion to be tracked for a short period of time. This observation is substantiated by tests where the wave propagates in the opposite direction. When the wave travels the opposite direction, it causes significant diesel to be pushed out of plane. This can be seen in nearly every test in both the small and large FOV imaging configurations.

3.2. Near-Field Liquid Fuel Jet Trajectory

The fuel spray trajectory from the liquid orifice affects penetration into the air crossflow and subsequent mixing and spreading across the detonation channel. Moreover, jets in crossflow in unsteady flowfields have been shown to deviate significantly from steady-state cases [10]. The fuel spray trajectory is determined by following the leading edge 15% intensity profile. First, an average is taken of the 40 images prior to the arrival of the detonation wave. The use of 40 images was chosen because it was observed that the spray is mostly fully recovered by this time (its trajectory and spray characteristics did not vary significantly with time). The leading edge spray profile (i.e., the fuel spray penetration) was then tabulated for the different test cases, as shown in Figure 5. For reference, penetration heights are compared with an experimentally-derived correlation for a spray injected from a bluff body into a subsonic crossflow (analogous to the current RDC configuration) [11], and shown in Equation 1.

$$y/d = (1.2+0.4d)q^{0.36}\ln[1+(1.56+0.48d)(x/d)] \quad (1)$$

where q is the momentum flux ratio between the air and the liquid diesel, d is the liquid orifice diameter, and x and y are the axial and radial trajectory

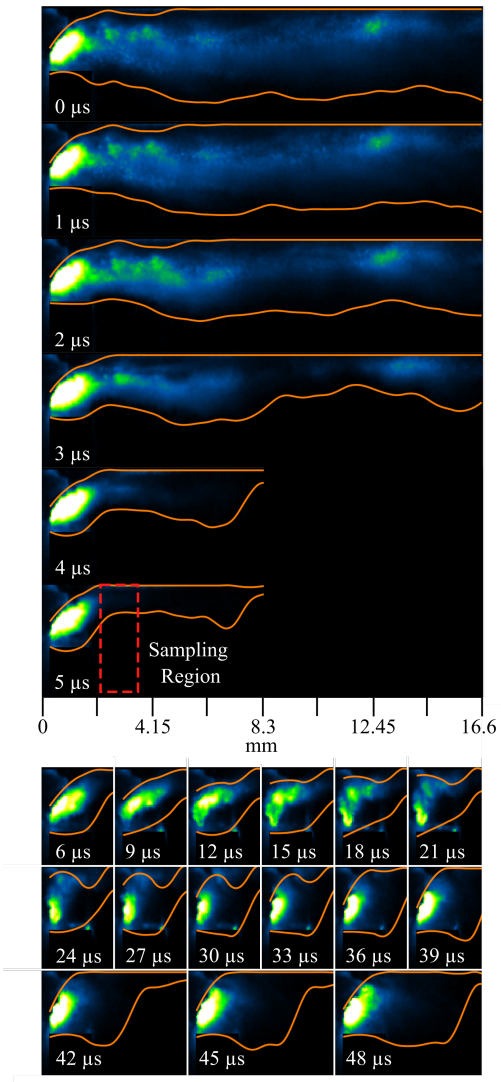

Fig. 4: Image sequence of diesel PLIF (small FOV, 1 MHz) for Case 1 around passage of the detonation wave. Time 6–48 μs are enhanced to highlight the spatio-temporal features of the unsteady fuel spray. The red box represents the sampling window that is used in the refill analysis.

coordinates. As shown in Figure 5, as liquid jet to air crossflow momentum flux ratio increases, near field fuel spray injection increases, as expected. The RDC fuel spray trajectory for q of 0.040 and 0.055 more closely follow the approximate shape of the correlation up until an axial distance of 4 mm. The cases with q of 0.013 and 0.030 do not appear to follow the correlation. Noticeably, there is a significant change in jet penetration after the backward facing step for cases with q of 0.013 and 0.030. This is also apparent

from the average of the 40 images prior to the arrival of the detonation wave, as shown in Figure 6. As q decreases, the fuel spray is entrained into the shear layer formed between the incoming reactants, and the wake formed behind the backward facing step. The axial velocity of the spray in the large FOV images was estimated by tracking flow features as they move downstream. At approximately 60 mm downstream the liquid velocity is on the order of 350 m/s. Similarly, for the small FOV image sequence in Figure 4, the liquid velocity is estimated to be 210 m/s at an axial distance of 3 mm.

3.3. Liquid Fuel Jet Recovery

Following the passage of the detonation wave, there is a temporary cessation of fuel spray entering the detonation channel. The refill time of the spray into the channel was characterized by sampling pixel intensity values in a region 2.1 mm by 4.6 mm located immediately downstream of the backward facing step (see Figure 3, ROI 1). Intensity profiles in time for this region of interest (ROI) are shown in Figure 7 for Cases 1, 4, and 5. The time at which the detonation wave arrives is marked by a dashed black vertical line. In general, the highest q has a shorter spray refill time compared with the lowest q. The refill time was calculated as the difference from wave arrival to when the spray PLIF signal in ROI 1 reached a value within 10% of a frame prior to wave arrival. Refill times for Cases 1–5 are shown in Table 2.

Alternatively, the overall recovery process can also be characterized by how quickly the leading edge of the spray returns to its approximate quasi-steady position immediately prior to the arrival of the detonation wave. For a single data set, the upper spray boundary line is averaged across 40 μs of images leading up to detonation wave arrival. A series of deviation values are calculated at each axial location by taking the difference between the averaged line and the instantaneous line. The deviation values are then averaged for each frame. Figure 8 shows an example of this method. In the test shown, the wave arrives at 42 μs. However, the leading edge of the jet remains undisturbed until 47 μs. At 100 μs it appears both in Figure 8 and the original images that the jet has largely recovered. As observed in Figure 3, the liquid jet penetration increases in the early period of recovery. Due to this, the leading edge of the spray has

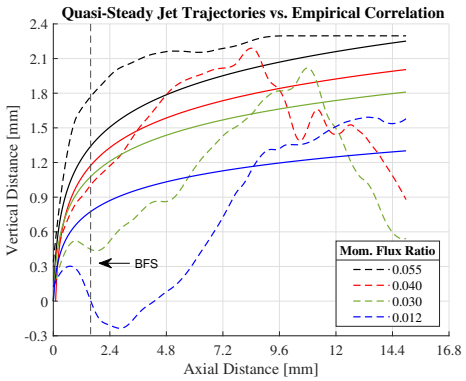

Fig. 5: Experimental penetration (dashed line) compared to empirical correlation (solid line) for various momentum flux ratios overlaid on a time-averaged images. From top to bottom, test cases are 1, 4, 2, and 3.

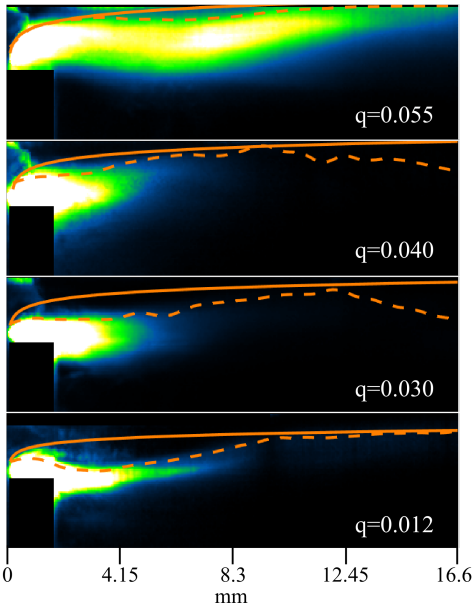

Fig. 6: Experimental penetration (dashed line) compared to empirical correlation (solid line) for various momentum flux ratios overlaid on a time-averaged images. From top to bottom, test cases are 1, 4, 2, and 3.

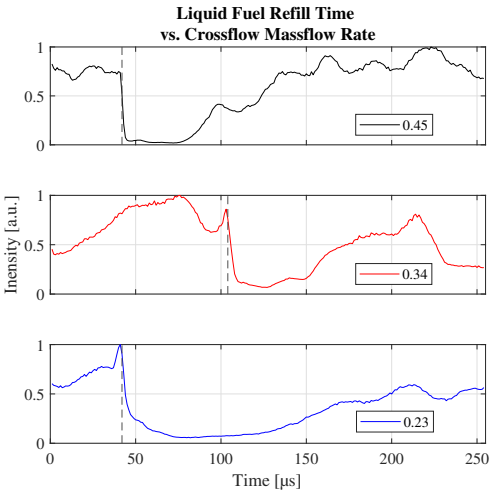

Fig. 7: Diesel PLIF signal recovery in the combustion channel as a function of time for varying air mass flow rates. From top to bottom, test cases are 1, 4 and 5.

Table 2: Average refill and jet recovery times

Test Case	Air $\dot{m}$ [kg/s]	Refill Time [μs]	Recovery Time [μs]
1	0.46	90	51
2	0.46	68	48
3	0.45	62	59
4	0.34	80	69
5	0.23	176	109

an increased penetration and thus an increased deviation. Similarly, the cases with air flow rates of 0.34 and 0.23 kg/s have a much more tapered recovery than cases with the higher flow rate of 0.45 kg/s. The results of both methodologies for characterizing fuel recovery are summarized in Table 2.

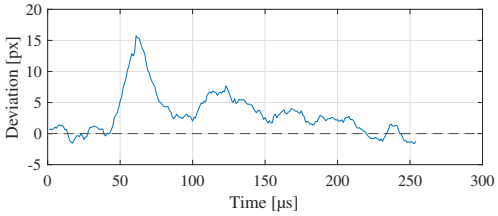

Fig. 8: Leading edge jet recovery as a function of time for test Case 1. Wave arrives at 42 μs.

4. Conclusion

The current work provides direct imaging of liquid fuel jet injection during the operation of an RDC. The RDC is operated on air and hydrogen to sustain a stable, cyclically propagating detonation wave, and one of the hydrogen fuel injection sites is replaced with a liquid jet to introduce a diesel spray that is visualized using burst-mode PLIF imaging up at rates of 200 kHz to 1 MHz. Conditions with various mass flow rates of liquid fuel and air were considered, with a range of liquid jet to air crossflow momentum flux ratios of 0.011–0.055. The time-resolved PLIF measurements reveal the evolution of the highly unsteady spray, as summarized below.

- *Spray development within a detonation period:* The jet recovery, breakup and entrainment into the supersonic crossflow of air, propagation into the detonation chamber, and interaction with the detonation wave is observed to occur within the detonation wave period ($\sim$275 μs for Case 1). Significant fuel spray stratification is observed across the channel, with the near field spray confined near the outer radius and the farfield spray occupying the entire radial depth of the channel. Tracking the spray front filling the channel shows spray velocities of up to 300–400 m/s. Spray development further down the channel suggests out-of-plane spray motion is occurring during the spray refill of the channel. Spray structures even further downstream also disappear well upstream of the detonation wave indicating improved mixing of the spray with the air near the end of the spray fill height
- *Liquid fuel trajectory:* As the injection system recovers, the fuel spray eventually returns to a quasi-steady position prior to the arrival of the subsequent detonation wave, allowing qualitative comparisons with theoretical jet trajectories for a range of air mass-flux conditions. For larger q, the trajectory agrees well with the correlation. For smaller q large differences are observed and attributed, in part, to the fuel spray entrained into the backward facing step shear layer.
- *Liquid fuel injection recovery:* Following passage of the detonation wave, the spray characteristics reveal significant changes in the momentum flux ratio between the liquid and air streams, altering the jet trajectory and temporarily halting fuel delivery to the detonation channel. For a fixed air mass flow rate (Cases 1–3), the temporary cessation of fuel spray injection into the combustor channel ranges from $\sim$20–30% of the detonation period, where lower q results in a faster recovery of the spray into the channel.

Acknowledgments

This work was funded by NASA STTR contract 80NSSC19C0551. Funding for some equipment was provided, in part, under AFOSR Award No. FA9550-16-1-0315 (Dr. Martin Schmidt, Program Officer) and DTRA Award No. HDTRA1-17-1-0031 (Dr. Jeffery Davis, Program Manager).

Supplementary material: None

References

[1] B. Rankin, C. Fugger, D. Richardson, K. Cho, J. Hoke, A. Caswell, J. Gord, F. Schauer, Evaluation of mixing processes in a non-premixed rotating detonation engine using acetone plif imaging, AIAA SciTech Conference (2016).

[2] Z. M. Ayers, A. I. Lemcherfi, E. W. Plaehn, T. R. Meyer, C. D. Slabaugh, C. A. Fugger, S. Roy, Application of 100 kHz Acetone-PLIF for the Investigation of Mixing Dynamics in a Self-Excited Linear Detonation Channel, in: AIAA Scitech 2021 Forum, 2021, p. 0554.

[3] F. Bykovski, S. Zhdan, E. Vedernikov, Continuous spin detonation of a heterogeneous kerosene–air mixture with addition of hydrogen, Combustion, Explosion, and Shock Waves 52 (3) (2016) 371–373. doi:10.2514/1.B37127.

[4] J. Kindracki, K. Wacko, P. Wozniak, S. Siatkowski, L. Mezyk, Influence of gaseous hydrogen addition on initiation of rotating detonation in liquid fuel–air mixtures, Energies (2020). doi:doi:10.3390/en13195101.

[5] H. Celebi, D. Lim, K. Dille, S. Heister, Response of angled and tapered liquid injectors to passing detonation fronts at high operating pressures, Shock Waves (2019).

[6] W. Anderson, S. Heister, Response of a liquid jet in a multiple-detonation driven crossflow, Journal of Propulsion and Power 35 (2) (2019) 303–312. doi:10.2514/1.B37127.

[7] P. S. Hsu, M. N. Slipchenko, N. Jiang, C. A. Fugger, A. M. Webb, V. Athmanathan, T. R. Meyer, S. Roy, Megahertz-rate oh planar laser-induced fluorescence imaging in a rotating detonation combustor, Optics Letters 45 (2020) 5776–5779.

[8] V. Athmanathan, . Braun, Z. Ayers, J. Fisher, C. Fugger, S. Roy, G. Paniagua, M. T.R, Detonation structure evolution in an optically-accessible non-premixed H2-Air RDC using MHz rate imaging, in: AIAA Scitech 2020 Forum, 2020.

[9] T. R. Meyer, M. Brear, J. R. Gord, Formation and diagnostics of sprays in combustion.

[10] A. R. Karagozian, Transverse jets and their control, Progress in Energy and Combustion Science 36 (2010) 531–553.

[11] C.-W. Lee, S. Moon, C.-H. Sohn, H.-J. Youn, Spray and combustion characteristics of a dump-type ramjet combustor, KSME International Journal 17 (12) (2003) 2019–2026. doi:10.1007/bf02982442.